Bioorganic & Medicinal Chemistry 19 (2011) 6274–6284

Contents lists available at SciVerse ScienceDirect

Bioorganic & Medicinal Chemistry

journal homepage: www.elsevier.com/locate/bmc

Improvement in oral bioavailability of 2,4-diaminopyrimidine c-Met inhibitors by incorporation of a 3-amidobenzazepin-2-one group

Karen L. Milkiewicz *, Lisa D. Aimone, Mark S. Albom, Thelma S. Angeles, Hong Chang, Jennifer V. Grobelny, Jean Husten, Christine LoSardo, Sheila Miknyoczki, Seetha Murthy, Damaris Rolon-Steele, Ted L. Underiner, Linda R. Weinberg, Candace S. Worrell, Kelli S. Zeigler, Bruce D. Dorsey

Worldwide Discovery Research, Cephalon, Inc. 145 Brandywine Parkway, West Chester, PA 19380-4245, USA

ARTICLE INFO

Article history:
Received 5 July 2011
Revised 30 August 2011
Accepted 6 September 2011
Available online 13 September 2011

Keywords:
c-Met
Kinase inhibitors
Oral bioavailability
PK-PD
In vivo efficacy

ABSTRACT

The hepatocyte growth factor (HGF)-c-Met signaling axis is involved in the mediation of many biological activities, including angiogenesis, proliferation, cell survival, cell motility, and morphogenesis. Dysregulation of c-Met signaling (e.g., overexpression or increased activation) is associated with the proliferation and metastasis of a wide range of tumor types, including breast, liver, lung, colorectal, gastric, bladder, and prostate, among others. Inhibiting the HGF-c-Met pathway is predicted to lead to anti-tumor effects in many cancers. Elaboration of the SAR around a series of 2,4-diaminopyrimidines led to a number of c-Met inhibitors in which pharmaceutical properties were modulated by substituents appended on the C2-benzazepinone ring. In particular, certain-3-amidobenzazepin-2-one analogs had improved oral bioavailability and were evaluated in PK/PD and efficacy models. Lead compounds demonstrated tumor stasis with partial regressions when evaluated in a GTL-16 tumor xenograft mouse model.

Under normal physiological conditions, during embryonic development, and hepatic and cardiac injury repair, the c-Met receptor tyrosine kinase and its high affinity ligand hepatocyte growth factor (HGF, also known as scatter factor) mediate a variety of cellular processes including proliferation, invasion, and angiogenesis.[1–4] In tumor cells, the activation of c-Met triggers a series of signaling cascades that results in cell growth, invasion, proliferation, and protection from apoptosis.[5,6] The over-expression of HGF and c-Met is associated with more aggressive tumors and poor patient prognosis.[7] Tumor biopsies of many solid tumors indicate expression of c-Met and HGF, and c-Met signaling has been noted in a wide range of malignancies, including breast, liver, lung, colorectal, gastric, bladder, prostate, head and neck, renal, pancreatic, sarcomas, thyroid, melanoma, and hematopoietic malignancies.[5,8,9] Activating mutations of c-Met have been identified in patients with hereditary forms of cancer, which directly implicates c-Met activation in human tumorogenesis.[10,11] Inhibition of c-Met kinase activity by small molecules would likely have broad therapeutic utility due to the prevalence of Met amplification/overexpression and mutations in a variety of human malignancies.[12] Many reports have indicated that the inhibition of c-Met kinase activity blocks tumor cell growth and invasion in both in vitro and in vivo systems.[13–17] There are many c-Met inhibitors in various stages of development.[18,19] Initial clinical results indicate that targeting the c-Met-HGF axis is tolerated and can lead to efficacious results either as single agent therapy or when combined with other tyrosine kinase inhibitors.[20,21]

As part of a c-Met discovery program, 2,4-diaminopyrimidines containing a C4-aminobenzamide group and a C2-aminobenzazepinone group (**1–3,** Table 1) that demonstrated potent c-Met inhibition and selectivity over a panel of other kinases were identified.[22] Analogs were evaluated for their inhibitory effects on the kinase activity of recombinant c-Met enzyme and on c-Met autophosphorylation in over-expressing human gastric carcinoma (GTL-16) cells. Counter-screening against the insulin receptor (IR) was also performed.[23] To assess kinase selectivity, select compounds were tested in the Ambit Bioscience KINOMEscan™;[24] these results are reported as S(90) values which reflect the fraction of kinases inhibited >90% when screened at 1 μM compound across a panel of >250 kinases.

The SAR of representative compounds from this series is reported in Table 1. Although these compounds demonstrated potent c-Met inhibitory activity in in vitro cellular assays, they suffered from poor systemic exposure and low oral bioavailability in rats. As described previously,[22] optimal compounds in this series all contained the 4-fluorobenzamide group as a means of balancing potency and kinase selectivity. Efforts to replace this fluorobenzamide moiety led to compounds with decreased potency and/or selectivity. Consequently, efforts to improve the pharmacokinetic (PK) properties of the series focused on optimizing the C2-benzazepinone portion of these analogs. Computer modeling studies suggested that the 2-benzazepinone occupied a solvent exposed

* Corresponding author. Tel.: +1 610 738 6823; fax: +1 610 344 0065.
E-mail address: kmilkiew@cephalon.com (K.L. Milkiewicz).

0968-0896/$ - see front matter © 2011 Elsevier Ltd. All rights reserved.
doi:10.1016/j.bmc.2011.09.006

Table 1
SAR of benzazepinone analogs **1–3**

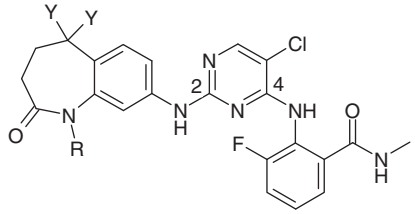

compd	Y	R	c-Met enzyme IC_{50}[a] (nM)	c-Met cell IC_{50}[a,b] (nM)	F[c] (%)
1	H	H	30	99	8
2	Me	H	54	10	1
3	Me	Et	10	44	0

[a] IC_{50} values are average of at least two separate determinations, see Experimental Section for assay conditions.
[b] GTL-16 cells.
[c] IV dosing 1 mg/kg, 1 mL/kg administered in 3% DMSO 30% Solutol, 67% PBS, oral dosing 5 mg/kg, 5 mL/kg administered in PEG400 in rat.

region, and thus might be amenable to modification with minimal impact on c-Met kinase activity (Fig. 1). Additionally, metabolic ID studies suggested that the C2-benzazepinone portion of the molecule was a target for oxidation, so functionalizing this portion of the molecule had a potential to decrease this metabolic liability.

Our initial strategy to improve oral bioavailability of these 2,4-diaminopyrimidine analogs involved appending amine functionality onto the C2-benzazepinone group of analog **2**. An amine substituent in this solvent exposed region could improve solubility of the molecule and potentially lead to more orally bioavailable compounds. Amino substituted benzazepinones are well known in the literature, aiming at a multitude of pharmaceutical targets, including PDK1 activators,[25] $Na_v1.7$ blockers,[26] thrombin inhibitors,[27] Factor Xa inhibitors,[28] calcium channel blockers,[29] cholecystokinin receptor ligands,[30] growth hormone secretagogues,[31] gastrin receptor antagonists,[32] endothelin-converting enzyme inhibitors,[33] and perhaps most notably, angiotensin converting enzyme inhibitors,[34] for example, benazepril. (Fig. 2)

The 3-aminobenzazepinones were prepared by a two-step iodination/amination sequence previously reported for other benzazepinones[35] and is illustrated in Scheme 1. Briefly, **4**[36] was sequentially treated with TMEDA, TMS-I, and then solid I_2 to afford iodo-intermediate **5**. After reaction with sodium azide, azido product **6** was then

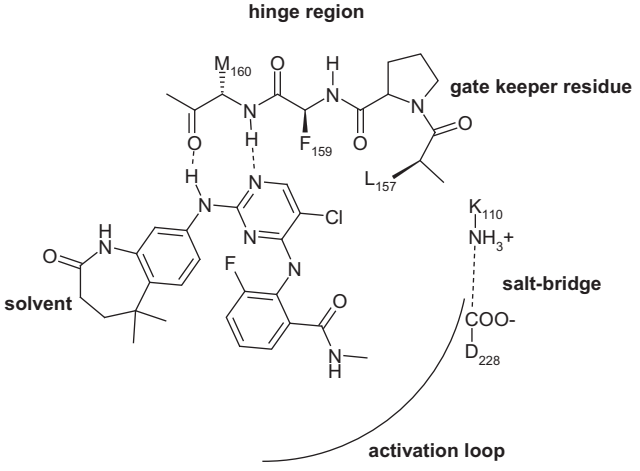

Figure 1. Depiction of **2** in the c-Met ATP-binding pocket.

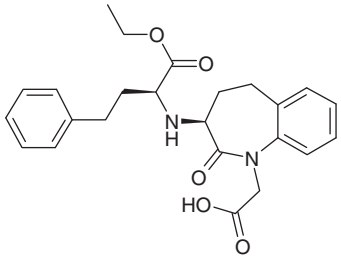

Figure 2. Benazepril, a known orally bioavailable aminobenzazepinone.

subjected to the Staudinger reduction[37] using polystyrene-triphenylphosphine in wet THF to afford aminobenzazepinone **7** in good yield. Attempts to directly displace the iodide of **5** with primary and secondary amines led predominantly to elimination rather than substitution products. After protecting benzazepinone **7** as its trifluoroacetamide **8a**, reduction of the nitro group with H_2/Pd afforded aniline **9a.** Utilizing previously reported chemistry,[38] this aniline was coupled to chloropyrimidine intermediate **10**. The resulting diaminopyrimidine–trifluoroacetamide **11** was saponified to afford amino-functionalized scaffold **12** (Scheme 1).

The SAR of diaminopyrimidine analogs **2**, **11** and **12** is summarized in Table 2 and shows that all three analogs possessed comparable c-Met GTL-16 cellular inhibitory activities. Although c-Met inhibition remained constant regardless of the benzazepinone substituent, amine analog **12** demonstrated more potent IR inhibition and lower kinase selectivity (i.e., larger S(90) value) than parent **2**. On the other hand, amide **11** showed greater selectivity over IR and demonstrated better kinase selectivity than either parent **2** or amine **12**. As predicted, amine **12** did achieve higher solubility than either parent **2** or trifluoroacetamide **11**. Amine **12** had a measured solubility of >120 μg/mL, whereas the solubility of **2** and **11** were 21 μg/mL and 8 μg/mL, respectively. In spite of the low solubility, trifluoroacetamide **11** demonstrated greater oral exposure than either **12** or **2** (Table 2). As a result of these unexpected data, a series of amidobenzazepinone analogs was synthesized in attempts to further improve the increased exposure seen with the trifluoroacetamide group. The goal with this series was to maintain c-Met cellular activity (cell IC_{50} <50 nM) and achieve oral exposures that would facilitate evaluation of analogs in PK/PD and anti-tumor efficacy models. Another objective in the program was to increase selectivity over IR (>50-fold), and improve kinase selectivity. An S(90) of <0.20 was desirable in order to reduce the potential for off-target liabilities.

Scheme 2 outlines the general synthesis of these amido-benzazepinone analogs. Acylation of amine **7** with acid chlorides afforded the corresponding amide intermediates **8b–f**, which upon hydrogenation yielded anilines **9b–f**. Finally, acid-catalyzed coupling of these anilines with aminopyrimidine **10**[36] led to the targeted diaminopyrimidines **13–17**.

A range of acylating partners were selected to yield amide, carbamate and urea products (**13–17**) and these are listed in Table 2. Initially, racemates were evaluated to determine which compounds might warrant further investigation as single enantiomers. As delineated in Table 2, all amide/urea/carbamate analogs (**11**, **13–17**) demonstrated comparable c-Met cell and enzyme inhibitory activity as parent **2**, but showed greater selectivity over IR and other kinases in the Ambit Bioscience KINOMEscan™ panel.

The PK properties (rat) of these functionalized, racemic benzazepinones were evaluated and pertinent data is listed in Table 2. Analogs **11**, **15**, **16**, and **17** all had markedly higher oral AUC values than initial lead compound **2**, leading to bioavailabilities ranging from 9–16% (as compared to 1%). It was therefore desirable to assess the

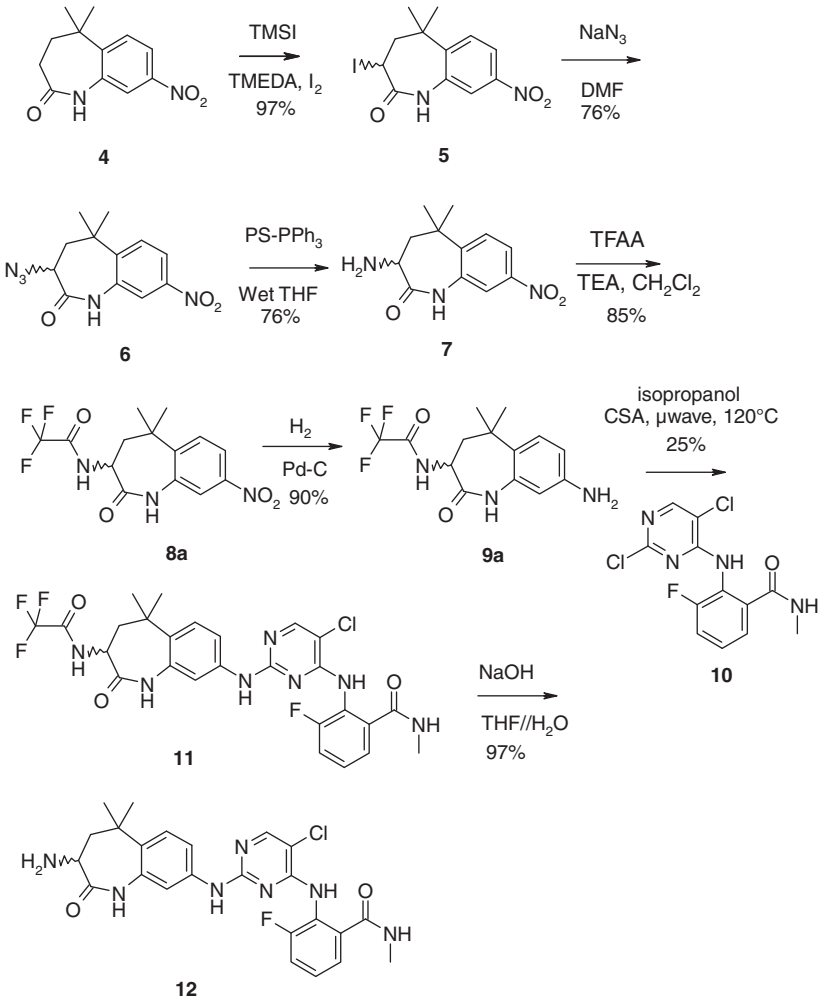

Scheme 1. Appendage of exocyclic amine on benzazepinone and synthesis of diaminopyrimidine analogs.

properties of the individual enantiomers associated with these racemates.

Resolution of racemates **11**, **15–17** was accomplished by supercritical fluid chromatography of either the final targets or intermediate **7**. In the latter case, both ***R*-7** and **S-7** were individually carried on to ***R*-12** and ***S*-12**, and ultimately converted to analogs ***R*-** and ***S*-11, 15–17**, respectively (Scheme 3). To determine absolute stereochemistry, a small molecule crystal structure of an acyl analog of **12** was solved. This analog was synthesized from the first eluting peak in the SFC separation of intermediate **7**. This allowed us to assign absolute stereochemistry to all compounds synthesized from both the first and second eluting peaks from the separation of **7**. The enantiomeric purities of all final compounds were then assessed by analytical chiral SFC.

Although the individual enantiomers **11**, **15–17**, had comparable c-Met cellular and enzymatic inhibitory activities, there were marked differences in kinase selectivity for *R*- and *S*-analogs (Table 3). In most cases, (compound **11** being the exception), the *S*-enantiomer was more selective than the *R*-enantiomer. For c-Met kinase, this region apparently has similar interactions with both enantiomers of **15–17**, whereas for other kinases, this region is more sensitive to the enantiotopic disposition of the amide, urea, or carbamate benzazepinone appendage. In general, these structurally related analogs shared similar kinase inhibitory profiles, largely targeting the same kinases (see Supplementary data for a comparison of enantiotopic profiles).

The *R* and *S* enantiomers of compound **16** were chosen for advanced studies due to the racemate's superior PK properties over other analogs (Table 2). The underlying reasons for the superior oral exposure (rat) of ***R*-16** over **2** are not clear (Table 2). Both analogs share similarly low pH 7.4 solubilities (26 vs 21 μg/mL, respectively), and comparably modest rat liver microsomal stability ($t_{1/2}$ = 21 vs 15 min).

The PK profiles of the single enantiomers were found to be identical. Interestingly, the bioavailability and AUC for the free base of racemate ***R*/*S*-16** (as well as each enantiomer, ***R*-16** and ***S*-16**) were greater than those for the corresponding trifluoroacetate salt of ***R*/*S*-16** (Table 4).

Because both ***R*** and ***S*-16** had reasonable oral bioavailability, both compounds were taken forward to PK-PD studies. A five day PK/PD study was conducted with ***R*** and ***S*-16** (10 and 30 mg/kg po, qd) to determine the plasma and tumor levels needed to inhibit c-Met phosphorylation in GTL-16 tumor xenografts (Figs. 3 and 4).

Even though administration of either ***R*-16** or ***S*-16** led to comparable plasma and tumor exposures, dosing ***R*-16** at 10 and 30 mg/kg, po, resulted in a greater PD response than dosing ***S*-16** (63–95% vs 53–77% c-Met inhibition at the 24 h time point). Furthermore, whereas c-Met inhibition remained relatively constant from 2–24 h post dosing of ***R*-16**, c-Met inhibition was more variable over the same period and less dose dependent upon treatment with ***S*-16**. At this time, reasons for this behavior are not evident and further studies are required to explain these observations.

Table 2
SAR and PK properties of functionalized benzazepinones

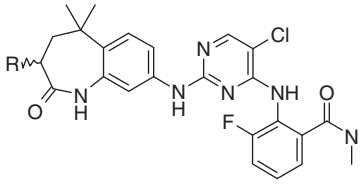

compd	R[a]	c-Met enzyme IC_{50} (nM)	c-Met cell IC_{50} (nM)[b]	IR IC_{50} (nM)	S(90)[c]	IV AUC (mg h/mL)[d]	Oral AUC (mg h/mL)[e]	Vd (L/kg)	CL (mL/min/kg)	*F* (%)
2	H	54	10	153	0.29	1057	46	0.5	16	1
11	CF_3CONH–	13	16	473	0.23	1311	606	1.2	16	9
12	NH_2	17	12	71	0.36	787	ND[f]	4.6	38	ND[f]
13	Me_2NCH_2CONH–	14	11	370	0.22	825	61	3.0	32	1
14	MeCONH–	22	18	3211	0.16	654	48	2.0	33	2
15	$MeOCH_2CONH$–	27	22	3111	0.14	846	497	1.3	20	12
16	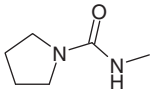	18	16	1729	0.16	3425	2631	0.8	6	15
17	MeOCONH–	28	20	886	0.21	1201	987	1.0	15	16

[a] Functionalized compounds **11, 13–17** were evaluated as mono-trifluoroacetic acid salts.
[b] GTL-16 cells.
[c] Kinase selectivity was determined using the Ambit Bioscience KINOMEscan™ technology.
[d] 1 mg/kg, 1 mL/kg IV administered in 3% DMSO 30% Solutol, 67% PBS in rats.
[e] 5 mg/kg, 5 mL/kg oral administered in 100% PEG400 in rats.
[f] ND = not determined—oral levels were too low to calculate.

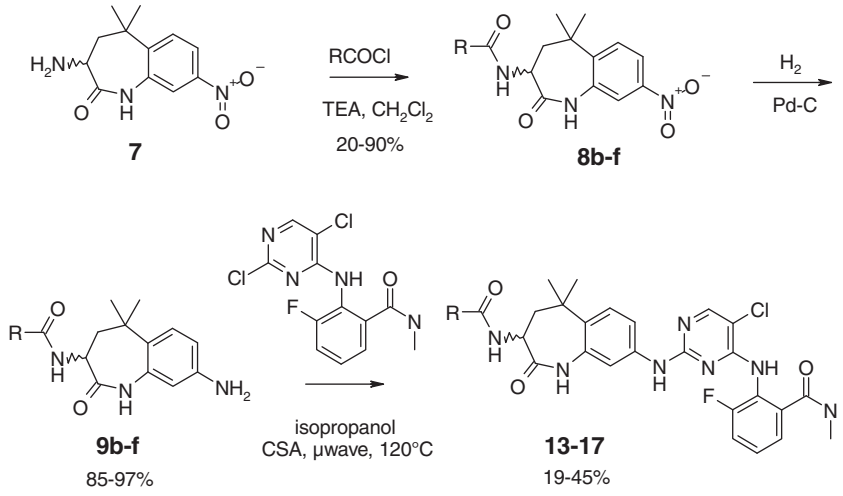

Scheme 2. Synthesis of amidobenzazepinones.

Based on the greater and more enduring c-Met inhibition demonstrated by ***R***- over ***S*-16**, the anti-tumor efficacy of ***R*-16** was evaluated in a GTL-16 tumor xenograft, murine model.

Administration of ***R*-16** at 10 and 30 mg/kg, po, bid and 100 mg/kg po, qd resulted in 70% ($p \leqslant 0.001$), 80% ($p \leqslant 0.001$) and 90% ($p \leqslant 0.001$) tumor growth inhibition, respectively. Initial tumor growth stasis [d 3–5 (10 and 30 mg/kg) or d 3–10 (100 mg/kg)] was followed by a short period of tumor growth followed by growth stasis between d 12 and 15 (Fig. 5). A follow-up study in this xenograft model confirmed this tumor growth inhibition pattern (data not shown).

In conclusion, appending an exocyclic amide or urea functionality onto a known benzazepinone 2,4-diaminopyrimidine c-Met inhibitor led to compounds with improved selectivity and oral bioavailability. Compounds with this functionality were identified that met program criteria: c-Met cellular activity <50 nM, selectivity over IR >50-fold, kinase selectivity S(90) <0.20 and oral exposure that would facilitate evaluation of analogs in PK/PD and anti-tumor efficacy models. In particular, analog ***R*-16** had a c-Met IC_{50} value of 16 nM in GTL-16 cells, 96-fold selectivity over IR, and a kinase selectivity S(90) value of 0.19 (68/353 kinases were inhibited greater than 90% at 1 μM, see Supplementary data for a complete list). Administration of ***R*-16** at 10 and 30 mg/kg, po, bid and 100 mg/kg po, qd, resulted in tumor growth inhibition, tumor growth stasis, and partial regressions in the c-Met dependent GTL-16 human gastric carcinoma xenograft model. Interestingly, while c-Met in vitro data and the PK data were comparable for the enantiomers of compound **16**, ***R*-16** demonstrated a stronger PK/PD response than its enantiomer, ***S*-16**. Efforts are underway to further evaluate how the nature of the amide functionality tethered to the benzazepinone affects the in vivo properties of this diaminopyrimidine series.

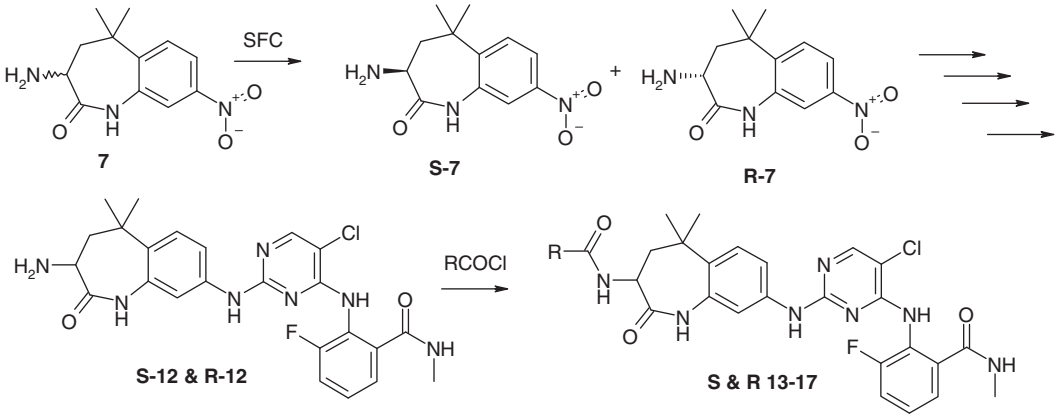

Scheme 3. Synthesis of ***R***- and ***S*-12–17**.

Table 3
SAR single enantiomer analogs ***R***- and ***S*-11**, **15**–**17**

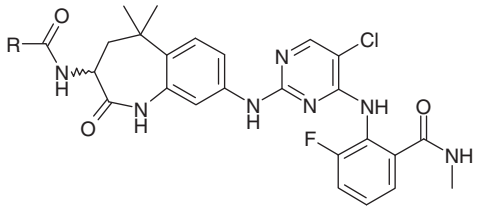

Compd	R	c-Met enzyme IC_{50} (nM)	c-Met cell IC_{50}[a] (nM)	IR IC_{50} (nM)	S(90)[b]
***R*/*S*-11**	CF_3–	13	16	473	0.23
***R*-11**	CF_3–	26	12	583	0.14
***S*-11**	CF_3–	38	17	945	0.24
***R*/*S*-15**	$MeOCH_2$–	27	22	3111	0.14
***R*-15**	$MeOCH_2$–	28	34	1807	0.21
***S*-15**	$MeOCH_2$–	37	26	2999	0.09
***R*/*S*-16**	Pyrrolidine–	18	16	1729	0.16
***R*-16**	Pyrrolidine–	24	26	1418	0.18
***S*-16**	Pyrrolidine–	70	34	2999	0.09
***R*/*S*-17**	MeO–	28	20	886	0.21
***R*-17**	MeO–	78	7	273	0.27
***S*-17**	MeO–	24	12	598	0.11

[a] GTL-16 cells.
[b] Kinase selectivity was determined using the Ambit Bioscience KINOMEscan™ technology.

1. Experimental

1.1. In vitro assays

c-Met activity assay. Example compounds were tested for their ability to inhibit the kinase activity of baculovirus-expressed c-Met using a modification of the assay protocol reported for trkA.[39] Phosphorylation of the substrate, phospholipase C-gamma (PLC-γ) generated as a fusion protein with glutathione *S*-transferase (GST) as reported,[40] was detected with a europium-labeled anti-phosphotyrosine antibody and measured by time-resolved fluorescence (TRF). Briefly, each 96-well plate was coated with 100 μL/well of 20 μg/mL substrate (PLC-γ) in Tris-buffered saline (TBS). The assay mixture (total volume = 100 μL/well) consisting of 50 mM HEPES (pH 7.2), 50 mM NaCl, 1 μM ATP (K_m level), 4 mM $MnCl_2$, 0.01% TritonX-100, and various concentrations of test compound (diluted in DMSO; 2.5% DMSO final in assay) was then added to the assay plate. The reaction was initiated by adding 10 ng/mL c-Met (cytoplasmic domain, in-house generated) and was allowed to proceed at room temperature for 30 min. Detection of the phosphorylated product was performed by adding 100 μL/well of Eu-N1 labeled PT66 antibody (PerkinElmer #AD0041; diluted 1:5000 in TBS containing 1% BSA). Incubation at 37 °C then proceeded for 1 h, followed by addition of 100 μL enhancement solution (PerkinElmer #1244-105). The plate was gently agitated and after 5–10 min, the fluorescence of the resulting solution was measured using the PerkinElmer EnVision® 2100 or 2102 multi-label plate reader. Data analysis was performed using ActivityBase (IDBS, Guildford, UK). IC_{50} values were calculated by plotting percent inhibition versus $\log_{10}$ of the concentration of compound and fitting to the non-linear regression sigmoidal dose-response (variable slope) equation in XLFit (IDBS, Guildford, UK).

The insulin receptor enzymatic screen was similar, with an assay mixture consisting of 20 mM HEPES (pH 7.2), 20 μM ATP, 5 mM $MnCl_2$ and 0.1% BSA. Enzyme (20 ng/mL βIR_{CD}) was added and the reaction was allowed to proceed at room temperature for 20 min. Detection of the phosphorylated product was performed by adding 100 μL/well of Eu-N1 labeled PY100 antibody (PerkinElmer #AD0160; diluted 1:10,000 in TBS-T containing 0.25% BSA). Incubation at 37 °C for 1 h was followed by addition

Table 4
Comparison of the PK properties of the individual enantiomers of compound **16**

Compd	IV AUC	Oral AUC	Vd (L/kg)	CL (mL/min/kg)	*F* (%)
***R*-16**	3460	5851	0.6	5	34
***S*-16**	3194	5548	0.6	5	35
***R/S*-16**	2331	4662	0.8	8	40
***R/S*-16 (TFA salt)**	3425	2631	0.8	6	15

of 50 μL enhancement solution (Wallace #1244-105). Plates were agitated for 10 min and the fluorescence was measured using the PerkinElmer EnVision® 2102 or 2104 multi-label plate reader.

GTL-16 cells (human gastric carcinoma cell line) were grown to about 85% confluency by seeding cells at 40,000 cells/well in 96-well, collagen 1-treated plates (Becton Dickinson #356407) a day before the experiment. Cells were washed 3X with TBS followed by addition of 100 μL/well of serum-free DMEM with 0.05% BSA (control). Test compounds were added and the plates were incubated for 2 h at 37 °C. Cells were washed at the end of incubation with deionized H_2O (3×) followed by addition of FRAK lysis buffer at 150 μL/well. The plates were then mixed for about 5 min and placed in a −80 °C freezer. Analysis of the samples for phosphorylated c-Met was performed using high-binding Greiner-Bio-One white assay plates (Greiner #655074) that were pre-coated with purified goat-anti-rabbit antibody ('Immunopure'; Pierce #31210; diluted 1:400 in TBS) followed by rabbit anti-c-Met antibody (VWR #71-8000; diluted 1:700 in TBS containing 1% BSA). The cell lysate plates were first thawed at 37 °C and spun down at 3500 rpm for about 10–15 min. For the capture step, lysates were transferred to the assay plates (100 μL/well) and incubated overnight at 4 °C. Plates were then washed 10× with deionized H_2O followed by a 2-hour incubation step with Eu-N1 labeled PY100 antibody (PerkinElmer #AD0160; diluted 1:2000 in TBS containing 1% BSA). After washing the plates 10× with water, 150 μL/well of enhancement solution (Wallace #1244-105) was added and the plates were read on the PerkinElmer EnVision® 2102 or 2104 multi-label plate reader.

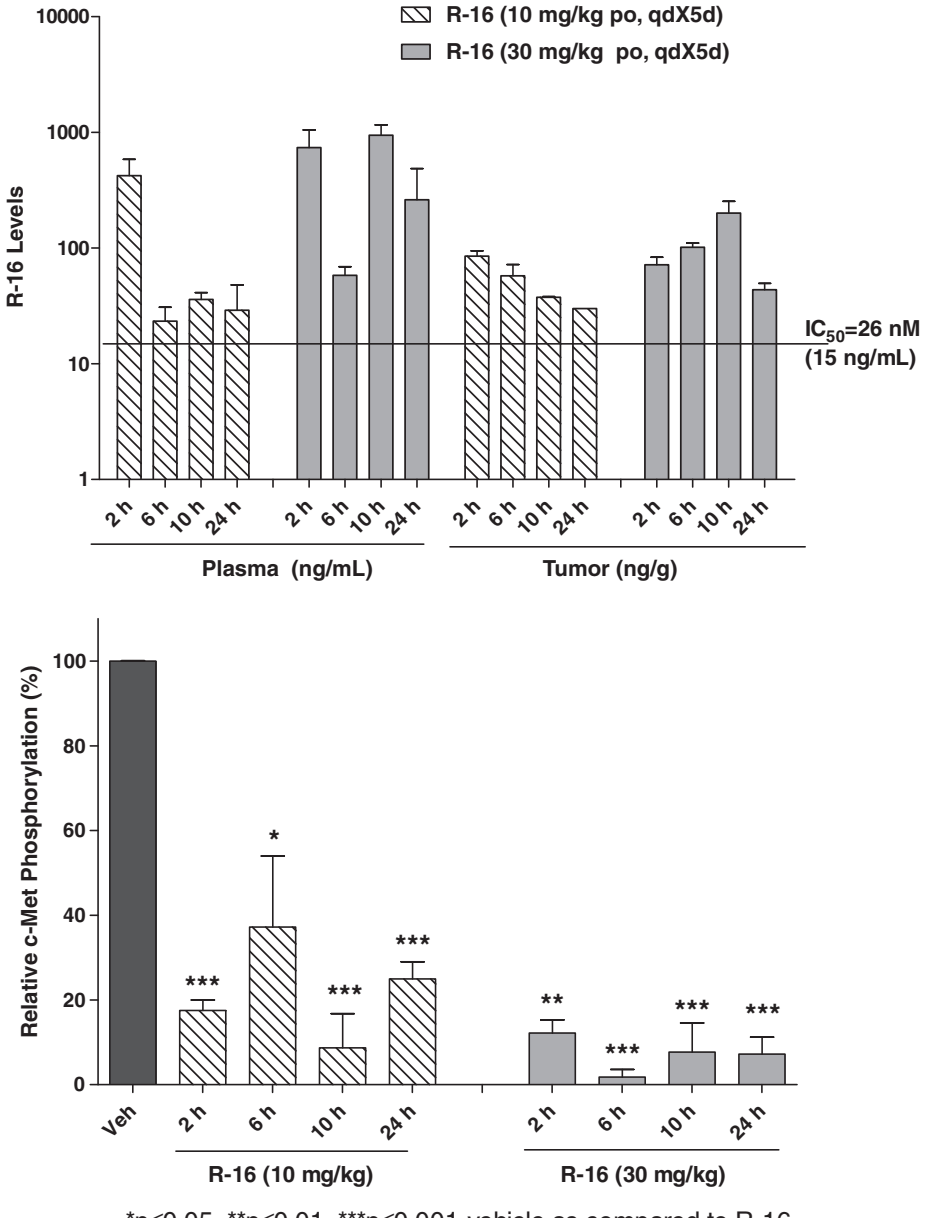

Figure 3. ***R*-16** PK/PD study.

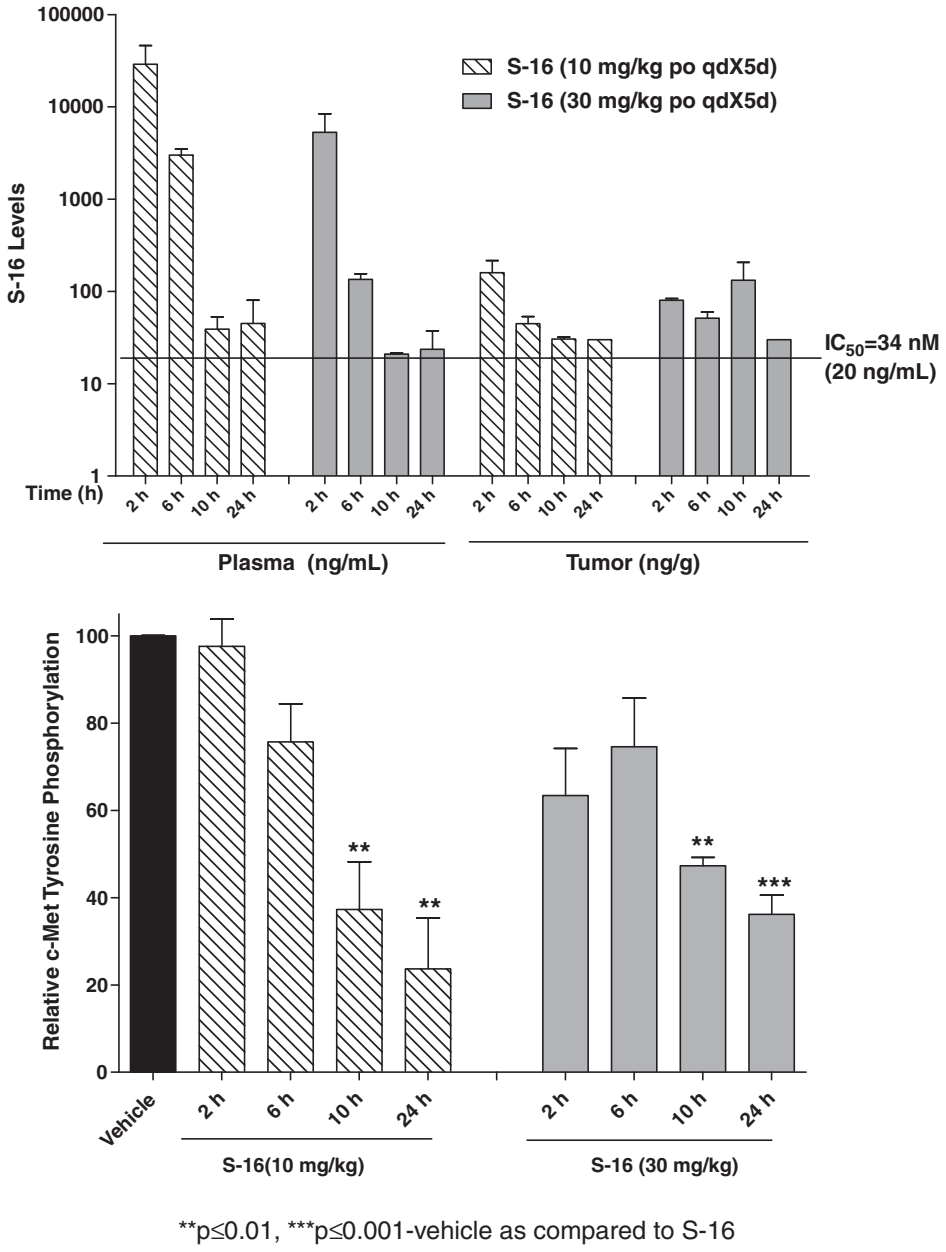

Figure 4. ***S-16*** PK/PD study.

1.2. Pharmacokinetic screening

Three adult male Sprague–Dawley rats were used in each treatment group. The rats were fasted overnight prior to oral dose administration. Intravenous administration was via the lateral tail vein and oral doses were administered by gavage. The compound was administered IV in a vehicle of 3% DMSO: 30% Solutol: 67% phosphate buffered saline. Oral dosing was in PEG400.

For blood collection, each rat (unanaesthetized) was placed in a clear Plexiglas® restraining tube, and blood samples (approximately 0.25 mL) were drawn from a lateral tail vein into heparinized collection tubes at predetermined sampling times (0.083, 0.25, 0.5, 1, 2, 4, and 6 h post dose). No pre-dose samples were obtained. The exception to this procedure was the last sampling time in which the animals were sacrificed by decapitation and trunk blood was obtained rather than blood via a tail vein. The blood samples were placed on wet ice until centrifuged to separate plasma. The plasma fraction was transferred into clean dry tubes, frozen on dry ice and stored at approximately −20 °C pending analysis.

Plasma was prepared for high performance liquid chromatography (HPLC)/mass spectrometric analysis according to standard protocol following protein precipitation with acetonitrile containing an internal standard. The plasma samples were then analyzed for both test compounds and alprenolol (internal standard) via HPLC coupled with tandem mass spectrometry.

The plasma concentration data for all rats were entered into Excel spreadsheets in preparation for pharmacokinetic analysis. Pharmacokinetic parameters for bortezomib were estimated for each rat by non-compartmental analysis (Gibaldi M, Perrier D. Pharmacokinetics, 2nd edition, Marcel Dekker, New York, Chapter 11, 1982) of the plasma concentration versus time data using WinNonlin software (Professional Version 4.1, Pharsight Corporation, Palo Alto, CA, 1997).

The maximum plasma concentration (C_{max}) was the highest observed plasma concentration after an oral dose; t_{max} was the corre-

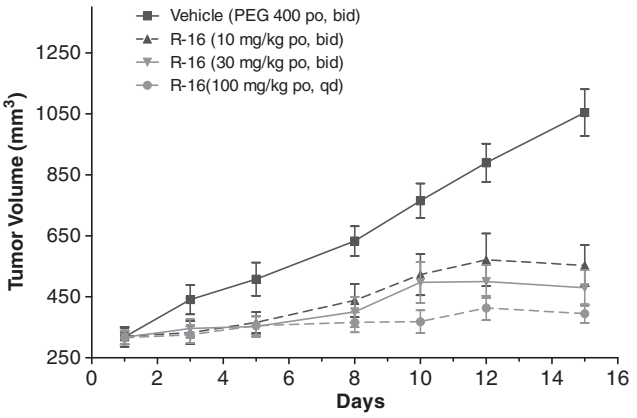

Day of Dosing	Vehicle vs. R-16-10 mg/kg bid	Vehicle vs. R-16-30 mg/kg bid	Vehicle vs. R-16-100 mg/kg qd
1	ns	ns	ns
3	ns	ns	p<0.05
5	p<0.05	p<0.05	p<0.05
8	p<0.01	p<0.01	p<0.001
10	p<0.05	p<0.01	p<0.0001
12	p<0.05	p<0.001	p<0.0001
15	p<0.001	p<0.001	p<0.0001

Figure 5. Anti-tumor efficacy of **R-16**.

sponding time when C_{max} was observed. The terminal rate constant for elimination from plasma (β) was estimated by linear regression of the terminal portion of the semi-logarithmic plasma concentration versus time curve. The apparent terminal half-life ($t_{1/2}$) was calculated as 0.693 divided by β. The area under the plasma concentration versus time curve from time zero to the time of the last measurable concentration (AUC_{0-t}) after a single dose was determined by the linear trapezoidal rule. The area from zero to infinity ($AUC_{0-\infty}$) was calculated as the sum of AUC_{0-t} and the area extrapolated from the last measurable concentration to infinity (C_{last}/β). Concentrations pre-dose were all assumed to be zero for the purpose of calculation of the AUC. Oral bioavailability was determined by dividing the dose normalized oral $AUC_{0-\infty}$ by the $AUC_{0-\infty}$ from IV dosing and multiplying by 100 to express the ratio as a percent.

1.3. Pharmacodynamic and anti-tumor efficacy studies

Compounds meeting the proposed selectivity, pharmacokinetic properties, and bioactivity in the previously mentioned assays underwent an initial scale-up for in vivo evaluation of anti-tumor activity. For the pharmacodynamic and anti-tumor efficacy studies, female athymic nude mice were injected with 1×10^6 GTL-16 human gastric carcinoma cells. Upon xenografts reaching a mean volume of 140 mm^3 mice were randomized into the appropriate treatment groups ($n = 3$ PK/PD study or $n = 10$ anti-tumor study). For the PK/PD studies mice were dosed for 5 d and were sacrificed at 2, 6, 10, and 24 h. Tumor lysates were analyzed for the inhibition of c-Met autophosphorylation or for determination of tumor compound levels by mass spectrometry along with the corresponding plasma and tissue samples. A commercially available ELISA (Biosource, Camarillo, CA) was used to evaluate the effects of c-Met inhibitors on c-Met phosphorylation. Tumors were homogenized in lysis buffer then incubated in a 96 well plate coated with anti-c-Met for 2 h. Plates were washed and then incubated with a phospho-c-Met antibody (Tyr1230/34/35) or total c-Met antibody for 1 h. Plates were washed and incubated with a anti-rabbit IgG-HRP antibody for 30 min. Tetramethylbenzidine was added to the wells and phosphorylation was quantitated by reading the absorbance on a microplate reader at 450 nm. Each sample was conducted in duplicate. The level of c-Met phosphorylation was normalized for total c-Met content.

For anti-tumor efficacy studies, mice were administered ***R*-16** over 3 concentrations for a two week period. Mice were weighed and tumor volumes determined every 2–3 days. Mice were monitored for signs of morbidity (behavior and body weight loss). At the termination of the study, tumors and plasma samples were taken for PK analysis.

All reagents and solvents were obtained from commercial sources and used as received. ^{1}H NMR spectra were obtained on a Bruker Avance at 400 MHz in the solvent indicated with tetramethylsilane as an internal standard. Analytical HPLC was run using a Zorbax Eclipse XDB-C8 3.5 μm 4.6 × 75 mm column eluting with a mixture of acetonitrile and water containing 0.1% trifluoroacetic acid with a 5 min gradient of 10–100%. LCMS results were obtained on either of two instruments. A Waters Acquity Ultra Performance LC with a Waters Aquity UPLC BEH C18 1.7 μm 2.1 × 50 mm column was paired with a Micromass-ZQ 2000 quadrupole mass spectrometer with electrospray ionization. Alternatively, an Agilent 1100 series HPLC with a Zorbax Eclipse XDB-C8 3.5 μm 2.1 × 30 mm column was paired with a Bruker Esquire 3000 mass spectrometer with electrospray ionization. Preparative HPLC was performed on a Gilson HPLC using a Phenomenex Gemini NX 5 μm C18, 21.2 × 100 mm column with UV detection. Supercritical Fluid Chromatography was performed on a AS-H Chiralpak column (10 × 250 mm, 5 μm), with a flow rate of 6 ml/min (35% MeOH, 0.1% DEA) at a pressure of 120 bar and a temperature of 35 °C. Automated column chromatography was performed on a CombiFlash Companion (Teledyne Isco Inc.). Melting points were taken on a Mel-Temp apparatus and are uncorrected.

Racemic samples were separated into the individual enantiomers using supercritical fluid chromatography on a chiralcel OJ-H column (250 × 4.6 mm, 5 μm) with 40% methanol. Spectral data for the single enantiomers were identical to that of the racemate.

1.3.1. 3-Iodo-5,5-dimethyl-8-nitro-1,3,4,5-tetrahydro-1-benzazepin-2-one (5)

5,5-Dimethyl-8-nitro-1,3,4,5-tetrahydro-benzo[*b*]azepin-2-one (**4**) (4.00 g, 17 mmol) in Methylene chloride (54 mL) was cooled to 0 °C and treated with *N*,*N*,*N*′,*N*′-tetramethylethylenediamine (7.73 mL, 51.2 mmol) then treated dropwise with iodotrimethylsilane (7.29 mL, 51.2 mmol). The mixture was stirred at 0 °C for 60 min after which solid Iodine (6.50 g, 25.6 mmol) was added in one portion and the mixture stirred at 0 °C for 60 min. The reaction was quenched with 10% $Na_2S_2O_3$ and filtered to recover a beige solid (2.63 g) The organic layer was diluted with EtOAc and washed with $Na_2S_2O_3$. The organic layer was dried over $MgSO_4$, filtered, and concentrated to a brown solid (1.80 g). The two solids were combined (5.43 g, 88%) LCMS 361 (M+H). The resulting solid was directly taken forward to the next step without purification.

1.3.2. 3-Azido-5,5-dimethyl-8-nitro-1,3,4,5-tetrahydro-1-benzazepin-2-one (6)

3-Iodo-5,5-dimethyl-8-nitro-1,3,4,5-tetrahydro-1-benzazepin-2-one (**5**) (5.37 g, 14.9 mmol), sodium azide (6.49 g, 100 mmol), and *N*,*N*-dimethylformamide (100 mL) were stirred at rt for 2 h. The reaction mixture was diluted with H_2O and the resulting beige ppt was filtered and taken to the next step without purification.

1.3.3. 3-Amino-5,5-dimethyl-8-nitro-1,3,4,5-tetrahydro-1 benzazepin-2-one (7)

3-Azido-5,5-dimethyl-8-nitro-1,3,4,5-tetrahydro-1-benzazepin -2-one (**6**) (3.10 g, 10.3 mmol), triphenylphosphine resin (1.0 mmol/g loading; 12 g, 11.55 mmol), tetrahydrofuran (120 mL) and water (0.9 mL) were combined and stirred at rt overnight. The reaction mixture was filtered and the resin was washed with MeOH. The

resulting solution was concentrated under reduced pressure and the resulting brown solid was triturated with CH_2Cl_2 to a beige solid. (HPLC purity >98%) ^{1}H NMR (DMSO-d_6, 400 MHz) δ 10.33 (br s, 1H), 8.00 (dd, J = 8.6 Hz, 1.7 Hz, 1H), 7.81 (d, J = 1.7 Hz, 1H), 7.66 (d, J = 8.6 Hz, 1H), 4.81 (dd, J = 7.5 Hz, 7.5 Hz, 1H), 2.71–2.66 (m, 1H), 2.61–2.55 (m, 1H), 1.39 (s, 3H), 1.35 (s, 3 H).

1.3.4. *N*-(5,5-Dimethyl-8-nitro-2-oxo-2,3,4,5-tetrahydro-1*H*-1-benzazepin-3-yl)-2,2,2-trifluoro-acetamide (8a)

Into a 1-neck round-bottom flask was added 3-amino-5,5-dimethyl-8-nitro-1,3,4,5-tetrahydro-1-benzazepin-2-one (**7**) (4.10 g, 16.4 mmol), methylene chloride (200 mL), pyridine (3.99 mL, 49.3 mmol), and trifluoroacetic anhydride (3.48 mL, 24.7 mmol). The reaction mixture was stirred at rt for 1 h. HPLC indicated complete conversion. The reaction mixture was washed with 10% citric acid to remove pyridine and the organic layer was dried over $MgSO_4$, filtered, and concentrated under reduced pressure. Product isolated as an off-white solid. ^{1}H NMR (DMSO-d_6, 400 MHz) δ 10.38 (br s, 1H), 9.69 (d, J = 7.88 Hz, 1H), 8.01 (dd, J = 8.66 Hz, 2.47 Hz, 1H), 7.87 (d, J = 2.47 Hz, 1H), 7.71 (d, J = 8.66 Hs, 1H), 4.35–4.28 (m, 1H), 2.30–2.27 (m, 2H), 1.47 (s, 3H), 1.35 (s, 3H).

1.3.5. *N*-(8-Amino-5,5-dimethyl-2-oxo-2,3,4,5-tetrahydro-1*H*-1-benzazepin-3-yl)-2,2,2-trifluoro-acetamide (9a)

N-(5,5-Dimethyl-8-nitro-2-oxo-2,3,4,5-tetrahydro-1*H*-1-benza zepin-3-yl)-2,2,2-trifluoro-acetamide (**8a**) (2.80 g, 8.1 mol), 10% palladium on carbon (50% Wet), 0.546 g, 0.25 mmol), and Methanol (7 mL) were combined in a Parr flask. The reaction mixture was shaken under an atmosphere of hydrogen (40 psi) for 90 min. The resulting mixture was filtered through Celite and the filtrate was concentrated to afford desired product as a white foam. LCMS 316.15 (M+H), H NMR ($CDCl_3$) δ 8.22, (s, 1H), 7.59 d, J = 6.1 Hz, 1H), 7.21 (d, J =8.5 Hz, 1H), 6.56 (dd, J = 1.0 Hz, 8.5 Hz, 1H), 6.31 (s, 1H), 4.58–4.52 (m, 1H), 3.75 (s, 2H), 2.64–2.59 (m, 1H), 1.92 (t, J = 12.1 Hz, 1H), 1.44 (s, 3H), 1.35 (s, 3H).

1.3.6. 2-{5-Chloro-2-[5,5-dimethyl-2-oxo-3-(2,2,2-trifluoro-acetylamino)-2,3,4,5-tetrahydro-1*H*-1-benzazepin-8-ylamino]-pyrimidin-4-ylamino}-3-fluoro-*N*-methyl-benzamide (11)

Into a 10 ml sealed tube was added *N*-(8-amino-5,5-dimethyl-2-oxo-2,3,4,5-tetrahydro-1*H*-1-benzazepin-3-yl)-2,2,2-trifluoro-acetamide (**9a**) (72 mg, 0.228 mmol), 2-(2,5-dichloro-pyrimidin-4 -ylamino)-3-fluoro-*N*-methyl-benzamide (**10**) (72 mg, 0.228 mmol), 10-camphorsulfonic acid (5.3 mg, 0.023 mmol) and isopropyl alcohol (2 mL). The reaction was heated under microwave radiation (300 watts) at 120 °C for 30 min. The title compound was isolated as a white solid after reverse phase HPLC and lyophilization (73 mg, 25%). HPLC purity 99%, LCMS 594.24 (M+H), ^{1}H NMR (DMSO-d_6, 400 MHz) δ 9.73 (s, 1H), 9.60 (d, J = 7.8 Hz, 1H), 9.43 (s, 1H), 9.37 (s, 1H), 8.50 (d, J = 4.5 Hz, 1H), 8.19 (s, 1H), 7.48–7.44 (m, 2H), 7.35–7.30 (m, 2H), 7.18 (s, 1H), 7.10 (d, J = 8.9 Hz, 1H), 4.27–4.20 (m, 1H), 2.73 (d, J = 4.2 Hz, 3H), 2.18–2.12 (m, 2H), 1.35 (s, 3H), 1.26 (s, 3H).

1.3.7. 2-[2-(3-Amino-5,5-dimethyl-2-oxo-2,3,4,5-tetrahydro-1*H*-1-benzazepin-8-ylamino)-5-chloro-pyrimidin-4-ylamino]-3-fluoro-*N*-methyl-benzamide (12)

2-{5-Chloro-2-[5,5-dimethyl-2-oxo-3-(2,2,2-trifluoro-acetyl-amino)-2,3,4,5-tetrahydro-1*H*-1-benzazepin-8-ylamino]-pyrimidin-4-ylamino}-3-fluoro-*N*-methyl-benzamide (**11**) (80 mg, 0.13 mmol) was dissolved in tetrahydrofuran (12 mL). 1.00 M of sodium hydroxide in water (2.4 mL) was added, and the reaction mixture was stirred at room temperature for 6 h, at which point HPLC indicated complete consumption of starting material. The reaction mixture was diluted with H_2O and extracted with CH_2Cl_2. The organic layer was dried over magnesium sulfate, filtered, and concentrated under reduced pressure to afford product as a white solid (66 mg, 97%). LCMS 498.22 (M+H), HPLC purity 94%, ^{1}H NMR ($CDCl_3$, 400 MHz) δ 8.90 (br s, 1H), 8.05 (s, 1H), 7.93 (br s, 1H), 7.63 (br s, 1H), 7.44–7.39 (m, 2H), 7.35–7.31 (m, 2H), 7.28–7.26 (m, 2H), 7.20 (d, J = 7.5 Hz, 1H), 6.90 (d, J = 8.2 Hz, 1H), 6.71 (br s, 1H), 3.40–3.37 (m, 1H), 2.93 (d, J = 4.7 Hz, 3H), 2.31–2.27 (m, 1H), 1.99–1.96 (m, 2H), 1.88–1.85 (m, 1H), 1.38 (s, 3H), 1.28 (s, 3H).

1.3.8. 2-{5-Chloro-2-[3-(2-dimethylamino-acetylamino)-5, 5-dimethyl-2-oxo-2,3,4,5-tetrahydro-1*H*-1-benzazepin-8-ylamino]-pyrimidin-4-ylamino}-3-fluoro-*N*-methyl-benzamide (13)

2-Dimethylamino-*N*-(5,5-dimethyl-8-nitro-2-oxo-2,3,4,5-tetrahydro-1*H*-1-benzazepin-3-yl)-acetamide (**8b**), dimethylamino-acetic acid (0.124 g, 1.20 mmol), EDCI (0.461 g, 2.41 mmol), HOBT (0.276 g, 2.05 mmol) and DMF(1.00 mL, 12.9 mmol) were stirred at rt for 30 min, followed by the addition of TEA (0.235 mL, 1.68 mmol) and 3-amino-5,5-dimethyl-8-nitro-1,3,4,5-tetrahydro-1-benzazepin-2-one **7** (0.300 g, 1.20 mmol). The reaction mixture was stirred at rt for 3 h, diluted with ether and washed with water. The organic layer was dried over $MgSO_4$, filtered, and concentrated under reduced pressure. Title compound was isolated as a white solid (80 mg, 20%).

1.3.9. *N*-(8-Amino-5,5-dimethyl-2-oxo-2,3,4,5-tetrahydro-1*H*-1-benzazepin-3-yl)-2-dimethylamino-acetamide (9b)

Title compound was prepared from 2-(2,5-dichloro-pyrimidin-4-ylamino)-3-fluoro-*N*-methyl-ben zamide (**10**) in an analogous manner to **11**. Title compound was isolated as a white solid. (55 mg, 45%). LCMS 585.30 (M+H), ^{1}H NMR (DMSO-d_6, 400 MHz) δ 9.67 (br s, 2H), 9.42 (s, 1H), 9.35 (s, 1H), 8.86 (d, J = 7.8 Hz, 1H), 8.50 (d, J = 4.9 Hz, 1H), 8.19 (s, 1H), 7.49–7.46 (m, 2H), 7.36–7.31 (m, 2H), 7.21 (s, 1H), 7.11 (d, J = 8.7 Hz, 1H), 3.93 (s, 2H), 2.78 (s, 6H), 2.74 (d, J = 4.1 Hz, 6H), 2.22–2.18 (m, 1H), 1.94–1.79 (m, 2H), 1.35 (s, 3H), 1.25 (s, 3H).

1.3.11. *N*-(5,5-Dimethyl-8-nitro-2-oxo-2,3,4,5-tetrahydro-1*H*-1-benzazepin-3-yl)-acetamide (8c)

Title compound was prepared from 3-amino-5,5-dimethyl-8-nitro-1,3,4,5-tetrahydro-1-benzazepin-2-one (**7**) and acetic anhydride in an analogous manner to **8a**. Title compound was isolated as a white solid. (420 mg, 90%), HPLC 99% purity, H NMR (DMSO-d_6) 10.21 (s, 1H), 8.14 (d, J = 7.8 Hz, 1H), 7.99 (d, J = 8.6 Hz, 1H), 7.84 (s, 1H), 7.69 (d, J = 8.7 Hz, 1H), 4.28–4.21 (m, 1H), 2.23–2.17 (m, 1H), 2.02–1.95 (m, 1H), 1.81 (s, 3H), 1.45 (s, 3H), 1.32 (s, 3H).

1.3.12. *N*-(8-Amino-5,5-dimethyl-2-oxo-2,3,4,5-tetrahydro-1*H*-1-benzazepin-3-yl)-acetamide (9c)

Title compound was prepared from *N*-(5,5-dimethyl-8-nitro-2-oxo-2,3,4,5-tetrahydro-1*H*-1-benzazepin-3-yl)-acetamide in an analogous manner to **9a**. (260 mg, 97%). HPLC purity = 90%, LCMS (262 (M+H). ^{1}H NMR (DMSO-d_6, 400 MHz) δ 9.59 (s, 1H), 7.98 (d, J = 8.0 Hz, 1H), 7.01 (d, J = 8.4 Hz, 1H), 6.38 (d, J = 8.3 Hz, 1H), 6.25 (s, 1H), 5.32 (br s, 2H), 4.26–4.22 (m, 1H), 2.06–2.00 (m, 1H), 1.80–1.77 (m, 1H), 1.77 (s, 3H), 1.29 (s, 3H), 1.21 (s, 3H).

1.3.13. 2-[2-(3-Acetylamino-5,5-dimethyl-2-oxo-2,3,4,5-tetrahydro-1*H*-1-benzazepin-8-ylamino)-5-chloro-pyrimidin-4-ylamino]-3-fluoro-*N*-methyl-benzamide (14)

Title compound was prepared from *N*-(5,5-dimethyl-8-nitro-2-oxo-2,3,4,5-tetrahydro-1*H*-1-benzazepin-3-yl)-acetamide and 2-(2,5-dichloro-pyrimidin-4-ylamino)-3-fluoro-*N*-methyl-benzamide (**10**) in an analogous manner to **11**. (62 mg, 43%). HPLC purity = 99%, LCMS 524 (M+H), ^{1}H NMR (DMSO-d_6, 400 MHz) δ 9.53 (s, 1H), 9.39 (s, 1H), 9.35 (s, 1H), 8.51 (d, J = 4.6 Hz, 1H), 8.19 (s, 1H), 8.04 (d, J = 8.0 Hz, 1H), 7.49–7.45 (m, 2H), 7.33–7.26 (m, 2H), 7.15 (s, 1H), 7.08 (d, J = 9.0 Hz, 1H), 4.22–4.17 (m, 1H), 2.73

(d, J = 4.4 Hz, 3H), 2.08–2.06 (m, 1H), 1.87–1.84 (m, 1H), 1.84 (s, 3H), 1.32 (s, 3H), 1.23 (s, 3H).

1.3.14. *N*-(5,5-Dimethyl-8-nitro-2-oxo-2,3,4,5-tetrahydro-1*H*-1-benzazepin-3-yl)-2-methoxy-acetamide (8d)

Title compound was prepared from 3-amino-5,5-dimethyl-8-nitro-1,3,4,5-tetrahydro-1-benzazepin-2-one (**7**) and methoxyacetyl chloride in an analogous manner to **8a**. (338 mg, 66%). HPLC purity = 99%, LCMS 250 (M+H), ^{1}H NMR (DMSO-d_6, 400 MHz) δ 10.33 (s, 1H), 8.00 (dd, J = 8.8 Hz, 2.0 Hz, 1H), 7.85 (d, J = 2.0 Hz, 1H), 7.82 (d, J = 7.8 Hz, 1H), 7.71 (d, J = 8.8 Hz, 1H), 4.30–4.27 (m, 1H), 3.80 (s, 2H), 3.31 (s, 3H), 2.27–2.24 (M, 1H), 2.10 (t, J = 13.4 Hz, 1H), 1.45 (s, 3H), 1.32 (s, 3H).

1.3.15. *N*-(8-Amino-5,5-dimethyl-2-oxo-2,3,4,5-tetrahydro-1*H*-1-benzazepin-3-yl)-2-methoxy-acetamide (9d)

Title compound was prepared from *N*-(5,5-dimethyl-8-nitro-2-oxo-2,3,4,5-tetrahydro-1*H*-1-benzazepin-3-yl)-2-methoxy-acetamide (**8d**) in an analogous manner to **9a**. (white foam, 170 mg, HPLC purity = 99%) LCMS 292 (M+H), ^{1}H NMR ($CDCl_3$, 400 MHz) δ 7.42 (d, J = 7.3 Hz, 1H), 7.30 (s, 1H), 7.20 (d, J = 8.4 Hz, 1H), 6.38 (s, 1H), 4.66–4.59 (m, 1H), 3.93–3.87 (m, 2H), 3.69 (br s, 2H), 3.43 (s, 3H), 2.56–2.51 (m, 1H), 1.91–1.85 (m, 1H), 1.42 (s, 3H), 1.35 (s, 3H),

1.3.16. 2-{5-Chloro-2-[3-(2-methoxy-acetylamino)-5,5-dimethyl-2-oxo-2,3,4,5-tetrahydro-1*H*-1-benzazepin-8-ylamino]-pyrimidin-4-ylamino}-3-fluoro-*N*-methyl-benzamide (15)

Title compound was prepared from *N*-(8-amino-5,5-dimethyl-2-oxo-2,3,4,5-tetrahydro-1*H*-1-benzazepin-3-yl)-2-methoxy-acetamide and 2-(2,5-dichloro-pyrimidin-4-ylamino)-3-fluoro-*N*-methyl-benzamide (**10**) in an analogous manner to **11**. Title compound was isolated as a white solid (40 mg, 38%) HPLC purity = 99%, LCMS = 572 (M+H), ^{1}H NMR (DMSO-d_6, 400 MHz) δ 9.72 (s, 1H), 9.40 (s, 1H), 9.34 (s, 1H), 8.51 (m, 1H), 8.18 (s, 1H), 7.70 (d, J = 7.8 Hz, 1H), 7.49–7.44 (m, 2H), 7.31–7.27 (m, 2H), 7.16 (s, 1H), 7.10 (d, 1H), 4.23–4.21 (m, 1H), 3.82 (s, 2H), 3.33 (s, 3H), 2.73 (d, J = 4.8 Hz, 3H), 2.22–2.18 (m, 1H), 1.92–1.88 (m, 1H), 1.33 (s, 3H), 1.24 (s, 3H).

1.3.17. Pyrrolidine-1-carboxylic acid (5,5-dimethyl-8-nitro-2-oxo-2,3,4,5-tetrahydro-1*H*-1-benzazepin-3-yl)-amide (8e)

Title compound was prepared from 3-amino-5,5-dimethyl-8-nitro-1,3,4,5-tetrahydro-1-benzazepin-2-one (**7**) and pyrrolidine-1-carbonyl chloride in an analogous manner to **8a**. Title compound was isolated as a pale yellow solid (256 mg, 92%). LCMS 347 (M+H). HPLC purity 99%.

1.3.18. Pyrrolidine-1-carboxylic acid (8-amino-5,5-dimethyl-2-oxo-2,3,4,5-tetrahydro-1*H*-1-benzazepin-3-yl)-amide (9e)

Title compound was prepared from pyrrolidine-1-carboxylic acid (5,5-dimethyl-8-nitro-2-oxo-2,3,4,5-tetrahydro-1*H*-1-benzazepin-3-yl)-amide (**8e**) in an analogous manner to **9a**. Title compound was isolated as a white solid, (140 mg, 85% yield). LCMS 317 (M+H), ^{1}H NMR ($CDCl_3$, 400 MHz) δ :7.52 (s, 1H), 7.17 (d, J = 8.3 Hz, 1H), 6.50 (d, J = 8.3 Hz, 1H), 6.25 (s, 1H), 5.27 (d, J = 6.6 Hz, 1H), 4.54–4.51 (m, 1H), 3.70 (s, 2H), 3.36–3.34 (m, 4H), 2.55–2.50 (m, 1H), 1.91–1.87 (m, 6H), 1.42 (s, 3H), 1.32 (s, 3H).

1.3.19. Pyrrolidine-1-carboxylic acid {8-[5-chloro-4-(2-fluoro-6-methylcarbamoyl-phenylamino)-pyrimidin-2-ylamino]-5,5-dimethyl-2-oxo-2,3,4,5-tetrahydro-1*H*-1-benzazepin-3-yl}-amide (16)

Title compound was prepared from pyrrolidine-1-carboxylic acid (8-amino-5,5-dimethyl-2-oxo-2,3,4,5-tetrahydro-1*H*-1-benzazepin-3-yl)-amide (**9e**) and 2-(2,5-dichloro-pyrimidin-4-ylamino)-3-fluoro-*N*-*N*-methyl-benzamide (**10**) in an analogous manner to **11**. Title compound was isolated as a white solid (29 mg, 22%), HPLC purity = 94%, LCMS 597 (M+H), ^{1}H NMR (DMSO-d_6, 400 MHz) δ 9.47 (s, 1H), 9.40 (s, 1H), 9.33 (s, 1H), 8.54 (d, 1H), 8.19 (s, 1H), 7.52–7.42 (m, 2H), 7.38–7.25 (m, 2H), 7.15–7.07 (m, 2H), 5.92 (m, 1H), 4.09 (m, 1H), 3.22–3.18 (m, 4H), 2.73 (d, J = 3.5 Hz, 3H), 1.81–1.77 (m, 4H), 1.32 (s, 3H), 1.23 (s, 3H).

1.3.20. (5,5-Dimethyl-8-nitro-2-oxo-2,3,4,5-tetrahydro-1*H*-1-benzazepin-3-yl)-carbamic acid methyl ester (8f)

Title compound was prepared from 3-amino-5,5-dimethyl-8-nitro-1,3,4,5-tetrahydro-1-benzazepin-2-one (**7**) and methyl chloroformate in an analogous manner to **8a**. Title compound is an off white solid. (94 mg, 38%) LCMS 308 (M+H).

1.3.21. (8-Amino-5,5-dimethyl-2-oxo-2,3,4,5-tetrahydro-1*H*-1-benzazepin-3-yl)-carbamic acid methyl ester (9f)

Title compound was prepared from (5,5-dimethyl-8-nitro-2-oxo-2,3,4,5-tetrahydro-1*H*-1-benzazepin-3-yl)-carbamic acid methyl ester in an analogous manner to **9a**. Title compound was isolated as a yellow solid (80 mg, 94%), LCMS 278 (M+H).

1.3.22. {8-[5-Chloro-4-(2-fluoro-6-methylcarbamoyl-phenylamino)-pyrimidin-2-ylamino]-5,5-dimethyl-2-oxo-2,3,4,5-tetrahydro-1*H*-1-benzazepin-3-yl}-carbamic acid methyl ester (17)

Title compound was prepared from (8-amino-5,5-dimethyl-2-oxo-2,3,4,5-tetrahydro-1*H*-1-benzazepin-3-yl)-carbamic acid methyl ester (**9f**) and 2-(2,5-dichloro-pyrimidin-4-ylamino)-3-fluoro-*N*-methyl-benzamide (**10**) in an analogous manner to **11**. Title compound was isolated as a pale yellow solid (30 mg, 19%) LCMS 558 (M+H), H NMR (DMSO-d_6) 9.51 (s, 1H), 9.39 (s, 1H), 9.34 (s, 1H), 8.51 (d, 1H), 8.19 (s, 1H), 7.49–7.46 (m, 2H), 7.39–7.25 (m, 3H), 7.15 (s, 1H), 7.09 (m, 1H), 3.93–3.90 (m, 1H), 3.50 (s, 3H), 2.74 (d, J = 3.8 Hz, 3H), 2.09–2.06 (m, 1H), 1.95–1.89 (m, 1H), 1.32 (s, 3H), 1.22 (s, 3H).

Acknowledgments

The authors would like to thank Mark Olsen and Emily Kordwitz for chiral separation of the racemates, and Rebecca Brown for bioanalysis.

Supplementary data

Supplementary data associated with this article can be found, in the online version, at doi:10.1016/j.bmc.2011.09.006.

References and notes

1. Nakamure, T.; Mizuno, S.; Matsumoto, K.; Sawa, Y.; Matsuda, H.; Nakamura, T. *J. Clin. Invest.* **2000**, *106*, 1511.
2. Comoglio, P. M.; Boccaccio, C. *Semin. Cancer Biol.* **2001**, *11*, 153.
3. Boccoccio, C.; Comoglio, P. M. *Nat. Rev. Cancer* **2006**, *6*, 637.
4. Huh, C. G.; Factor, V. M.; Sanchez, A.; Uchida, K.; Conner, E. A.; Thorgeirsson, S. S. *Proc. Natl. Acad. Sci. U.S.A.* **2004**, *101*, 4477.
5. Birchmeier, C.; Birchmeier, W.; Gherardi, E.; VandeWoude, G. F. *Nat. Rev. Mol. Cell Biol.* **2003**, *4*, 915.
6. Liu, X.; Yao, W.; Newton, R. C.; Scherle, P. A. *Expert Opin. Investig. Drugs* **2008**, *17*, 997.
7. Boccaccio, C.; Comoglio, P. M. *Nat. Rev. Cancer* **2006**, *6*, 637.
8. Trusolino, L.; Comoglio, P. M. *Nat. Rev. Cancer* **2002**, *2*, 289.
9. Peruzzi, B.; Bottaor, D. P. *Clin. Cancer Res.* **2006**, *12*, 3657.
10. Schmidt, L.; Duh, F. M.; Chen, F., et al *Nat. Genet.* **1997**, *16*, 68.
11. Jeffers, M.; Schmidt, L.; Nakaigawa, N., et al *Proc. Natl. Acad. Sci. U.S.A.* **1997**, *94*, 11445.
12. Peruzzi, B.; Bottaro, D. P. *Clin. Cancer Res.* **2006**, *12*, 3657.

13. Wang, X.; Le, P.; Liang, C.; Chan, J.; Kiewlich, D.; Miller, T.; Harris, D.; Sun, L.; Rice, A.; Vasile, S.; Black, R. A.; Howlett, A. R.; Patel, N.; McMahon, G.; Lipson, K. E. *Mol. Cancer Ther.* **2003**, *2*, 1085.
14. Sattler, M.; Pride, Y. B.; Ma, P.; Gramlich, J. L.; Chu, S. C.; Quinnan, L. A.; Shirazian, S.; Liang, C.; Podar, K.; Christensen, J. M.; Salgia, R. *Cancer Res.* **2003**, *63*, 5462.
15. Christensen, J. G.; Schreck, R.; Burrows, J.; Kuruganti, P.; Chan, E.; Le, P.; Chen, J.; Wang, X.; Ruslim, L.; Blake, R.; Lipson, K. E.; Ramphal, J.; Do, S.; Cui, J. J.; Cherrington, J. M.; Mendel, D. B. *Cancer Res.* **2003**, *63*, 7345.
16. Hov, H.; Holt, R. U.; Ro, T. B.; Fagerli, U.-M.; Hjorth-Hansen, H.; Baykov, V.; Christensen, J. G.; Waage, A.; Sundan, A.; Borset, M. *Clin. Cancer Res.* **2004**, *10*, 6686.
17. Zou, H. Y.; Li, Q.; Lee, J. H.; Arango, M. E.; McDonnell, S. R.; Yamazaki, S.; Koudriakova, T. B.; Alton, G.; Cui, J. J.; Kung, P.-P.; Nambu, M. D.; Los, G.; Bender, S. L.; Mroczkowski, B.; Christensen, J. G. *Cancer Res.* **2007**, *67*, 4408.
18. Underiner, T. L.; Herbertz, T.; Miknyoczki, S. J. *Anti-Cancer Agents Med. Chem.* **2010**, *10*, 7.
19. Porter, J. *Expert Opin. Ther. Pat.* **2010**, *20*, 159.
20. Stabile, L. P.; Rothstein, M. E.; Keohavong, P.; Lenzner, D.; Land, S. R.; Gaither-Davis, A. L.; Kim, K. J.; Kaminski, N.; Siegfried, J. M. *Cancers* **2010**, *2*, 2153.
21. Zhang, Y.; Staal, B.; Essenburg, C.; Su, Y.; Kang, L.; West, R.; Kaufman, D.; DeKoning, T.; Eagleson, B.; Buchanan, S. G.; Vande Woude, G. F. *Cancer Res.* **2010**, *70*, 6880.
22. Weinberg, L. R.; Albom, M. S.; Angeles, T. S.; Husten, J.; Lisko, J. G.; McHugh, R. J.; Milkiewicz, K. L.; Murthy, S.; Ott, G. R.; Theroff, J. P.; Tripathy, R.; Underiner, T. L.; Zificsak, C. A.; Dorsey, B. D. *Bioorg. Med. Chem. Lett.* **2011**, *21*, 164.
23. As a key regulator of glucose metabolism, selectivity against IR was desired to be >10-fold in the enzymatic assays.
24. Fabian, M. A.; Biggs, W. H., III; Treiber, D. K.; Atteridge, C. R.; Azimioara, M. D.; Benedetti, M. G.; Carter, T. A.; Ciceri, P.; Edeen, P. T.; Floyd, M.; Ford, J. M.; Galvin, M.; Gerlach, J. L.; Grotzfeld, R. M.; Herrgard, S.; Insko, D. E.; Insko, M. A.; Lai, A. G.; Lelias, J.-M.; Mehta, S. A.; Milanov, Z. V.; Velasco, A. M.; Wodicka, L. M.; Patel, H. K.; Zarrinkar, P. P.; Lockhart, D. *J. Nat. Biotechnol.* **2005**, *23*, 329.
25. Wei, L.; Gao, X.; Warne, R.; Hao, X.; Bussiere, D.; Gu, X.; Uno, T.; Liu, Y. *Bioorg. Med. Chem. Lett.* **2010**, *20*, 3891.
26. Hoyt, S. B.; London, C.; Ok, H.; Gonzalez, E.; Duffy, J. L.; Abbadie, C.; Dean, B.; Felix, J. P.; Garcia, M. L.; Jochnowitz, N., et al *Bioorg. Med. Chem. Lett.* **2007**, *17*, 6172.
27. Ho, J. Z.; Gibson, T. S.; Semple, J. E. *Bioorg. Med. Chem. Lett.* **2002**, *12*, 743.
28. Tamura, S. Y.; Goldman, E. A.; Bergum, P. W.; Semple, J. E. *Bioorg. Med. Chem. Lett.* **1999**, *9*, 2573.
29. Kimball, S. D.; Floyd, D. M.; Das, J.; Hunt, J. T.; Krapcho, J.; Rovnyak, G.; Duff, K. J.; Lee, V. G.; Moquin, R. V. *J. Med. Chem.* **1992**, *35*, 780.
30. Lowe, J. A., III; Hageman, D. L.; Drozda, S. E.; McLean, S.; Bryce, D. K.; Crawford, R. T.; Zorn, S.; Morrone, J.; Bordner, J. *J. Med. Chem.* **1994**, *37*, 3789.
31. Schoen, W. R.; Pisano, J. M.; Prendergast, K.; Wyvratt, M. J., Jr.; Fisher, M. H.; Cheng, K.; Chan, W. W.-S.; Butler, B.; Smith, R. G.; Ball, R. G. *J. Med. Chem.* **1994**, *37*, 897.
32. Kawanishi, Y.; Ishihara, S.; Tsushima, T.; Seno, K.; Hagishita, S.; Ishikawa, M.; Ishihara, Y. *Bioorg. Med. Chem.* **1997**, *5*, 1411.
33. Wallace, E. M.; Moliterni, J. A.; Moskal, M. A.; Neubert, A. D.; Marcopulos, N.; Stamford, L. B.; Trapani, A. J.; Savage, P.; Chou, M.; Jeng, A. Y. *J. Med. Chem.* **1998**, *41*, 1513.
34. Watthey, J. W.; Stanton, J. L.; Desai, M.; Babiarz, J. E.; Finn, B. M. *J. Med. Chem.* **1985**, *28*, 1511.
35. Zheng, N.; Armstrong, J. D.; Eng, K. K.; Keller, J.; Liu, T.; Lynch, R. J.; Hartner, F. W.; Volante, R. P. *Tetrahedron: Asymmetry* **2003**, *14*, 3435–3446.
36. Synthesis described in Ref. [22] (Weinberg, et al.)
37. Staudinger, H.; Meyer, J. *Helv. Chim. Acta* **1919**, *2*, 635.
38. Synthesis described in Ref. [22] (Weinberg, et al.)
39. Angeles, T. S.; Steffler, C.; Bartlett, B. A.; Hudkins, R. L.; Stephens, R. M.; Kaplan, D. R.; Dionne, C. A. *Anal. Biochem.* **1996**, *236*, 49.
40. Rotin, D.; Margolis, B.; Mohammadi, M.; Daly, R. J.; Daum, G.; Li, N.; Fischer, E. H.; Burgess, W. H.; Ullrich, A.; Schlessinger, J. *EMBO J.* **1992**, *11*, 559.